

PAPER • OPEN ACCESS

Effect of 200 MeV Ag¹⁶⁺ swift heavy ion irradiation on structural and magnetic properties of M-type barium hexaferrite

To cite this article: G Packiaraj *et al* 2019 *Mater. Res. Express* **7** 016301

View the [article online](#) for updates and enhancements.



LIVE AWARDS AND SPECIAL EVENTS

PLENARY LECTURE:
"Perovskite Solar Cells: Past 10 Years and Next 10 Years" with *Nam-Gyu Park*

LEGENDS OF BATTERY SCIENCE:
A Celebration with *M. Stanley Whittingham* and *Akira Yoshino*





PRiME
PACIFIC RIM MEETING
ON ELECTROCHEMICAL
AND SOLID STATE SCIENCE
2020

**ATTENDEES
REGISTER FOR FREE ▶**

PRiME 2020 • October 4-9, 2020
Hosted daily: 2000h ET & 0900h JST/KST

Materials Research Express



PAPER

OPEN ACCESS

RECEIVED

8 October 2019

REVISED

29 October 2019

ACCEPTED FOR PUBLICATION

31 October 2019

PUBLISHED

11 November 2019

Original content from this work may be used under the terms of the [Creative Commons Attribution 3.0 licence](#).

Any further distribution of this work must maintain attribution to the author(s) and the title of the work, journal citation and DOI.



Effect of 200 MeV Ag^{16+} swift heavy ion irradiation on structural and magnetic properties of M-type barium hexaferrite

G Packiaraj¹, K Sakthipandi² and Aslam Hossain³

¹ Department of Physics, Aditya College of Engineering, Surampalem 533 437, Andhra Pradesh, India

² Department of Physics, Sethu Institute of Technology, Kariapatti 626 115, Tamil Nadu, India

³ Department of Physical and Inorganic Chemistry, Institute of Natural Sciences and Mathematics, Ural Federal University Yekaterinburg, Russia

E-mail: sakthipandi@gmail.com

Keywords: barium hexaferrite, Sol Gel method, swift heavy ion irradiation, structural properties, magnetic properties

Abstract

M-type barium hexagonal ferrite ($\text{BaFe}_{12}\text{O}_{19}$) has been synthesized by sol-gel auto combustion method. The synthesized material was irradiated with 200 MeV Ag^{16+} ions using the 15UD Pelletron tandem accelerator and the changes in structural and surface morphology of material were investigated. The pristine (as-synthesised) and irradiated samples were characterized using different experimental techniques like x-ray diffraction (XRD), Fourier-transform infrared spectroscopy, transmission electron microscope (TEM) and vibrating sample magnetometer (VSM). The strong absorption peak between 580 and 440 cm^{-1} in the infrared spectrum and XRD confirmed the formation of ferrite structure for both irradiated and pristine samples. XRD peaks for the irradiated barium hexagonal ferrite were slightly broadened when compared pristine ferrite samples. The crystallite size of the irradiated barium hexagonal ferrite was higher than that of pristine barium hexagonal ferrite and is consistent with TEM images. Both saturation magnetization and coercivity were decreased with irradiation.

1. Introduction

Since last two decades, effects of Swift heavy ion irradiation on magnetic oxides and ferrites have been investigated to understand the modifications on their physical, magnetic and dielectric properties [1–3]. This is an establish phenomenon that irradiation of solids with energetic particle beams could be able to create an extensive variation of defect states. It is possible for some materials to create additional defects and phase transformations to anisotropic growth, using various range (MeV) of swift heavy ions radiation [4]. The material with swift heavy ion irradiation is an important tool which would be able to manipulate the properties of materials. This could provide an alternative to photons for presenting electronic excitations to material [5].

The wide application of hexagonal ferrites attracted the attention of researchers due to its technological applications in electronic and magnetic devices [6, 7]. Different research group has been tried to tune the magnetic anisotropy of M-type strontium hexaferrite crystals by the swift heavy ion irradiation [1, 8, 9]. Panchal *et al* [10] reported effect of swift heavy ion irradiation on structural and magnetic properties of strontium hexaferrites where the intensity of all the peaks and FWHM were increased. M-type $\text{BaFe}_{12}\text{O}_{19}$ has special identity due to its application as permanent magnets [11, 12].

The increasing current demand of low cost, excellent chemically stable and corrosion resistive M-type $\text{BaFe}_{12}\text{O}_{19}$ was further studied for microwave communication, microwave dark room, the anti-electromagnetic wave radiation applications [13, 14]. In this purpose, we synthesized M-type barium hexagonal ferrite ($\text{BaFe}_{12}\text{O}_{19}$) and to tune the structural and magnetic properties irradiated by swift heavy ion irradiation.

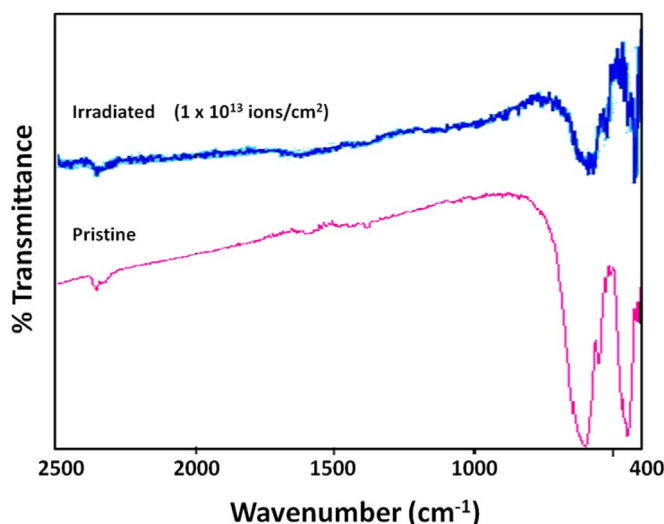


Figure 1. FTIR spectra of pristine and irradiated $\text{BaFe}_{12}\text{O}_{19}$ powder.

2. Experimental procedure

Barium nitrate $\text{Ba}(\text{NO}_3)_2$ (Merck, GR grade), iron nitrate $\text{Fe}(\text{NO}_3)_3 \cdot 9\text{H}_2\text{O}$ (Sigma Aldrich, >98% purity) were used as precursor materials. Firstly, all of the materials with specific amount were dissolved into distilled water to produce the target product, $\text{BaFe}_{12}\text{O}_{19}$. Citric acid $\text{C}_6\text{H}_8\text{O}_7$ (Merck, GR grade) as combustion fuel was then added and aqueous solution of NH_4OH (Merck, GR grade) was used drop wise to maintain the pH to 7. After that the solution was heated on a hot plate at 80–90 °C to evaporate the remaining water. Finally, the solution was turned into a viscous gel and the gel was self-ignited and burnt. The ash form of the product is crushed and preheated for 500 °C followed by final calcinations at 950 °C for 4 h. Thus, the prepared barium hexagonal ferrite was irradiated with 200 MeV Ag^{16+} ions at a fluence of $1 \times 10^{13} \text{ ions cm}^{-2}$ using 15UD Pelletron Accelerator at New Delhi Inter University Accelerator Centre (IUAC), India. TRIM/SRIM calculations was used to calculate the electronic energy loss, nuclear energy loss in range of the 200 MeV Ag^{16+} ion beam [15].

Both pristine and irradiated barium hexagonal ferrites were characterized using different experimental techniques like x-ray diffraction (XRD), Fourier-transform infrared spectroscopy, transmission electron microscope (TEM) and vibrating sample magnetometer (VSM). XRD spectrum was recorded by SEIFERT XRD 3000 PTS between the diffraction angle (2θ) from 20° to 80° using CuK_α ($\lambda = 1.5405 \text{ \AA}$) as a radiation source. FTIR was taken at room temperature in the wavenumber range from 4000 to 400 cm^{-1} using FTIR Brucker tensor-27 spectrometer. The particle size of pristine and irradiated hexagonal ferrites was examined through a scanning electron microscope (Philips, CM 200, USA). Field-dependent magnetization was recorded using vibrating sample magnetometer (VSM: EG & G Princeton Applied Research, Model 4500) with a maximum field of 15 KOe.

3. Results and discussion

FTIR spectra of pristine and irradiated barium hexaferrite samples is shown in figure 1. Two absorption bands at 580 and 440 cm^{-1} were observed in both pristine and irradiated barium hexaferrite samples. These bands correspond to vibrations of the intermetallic bond between the metal-oxygen ions. It is noted that the intensity of these bands is found to decrease in the irradiated sample when compared to the pristine barium hexaferrite sample. The excited dipole moments in the sample originated from molecular vibrations is responsible for the occurrence of the peak in the FTIR spectrum. The decrease in intensity for IR Spectrum of irradiated sample may be due to shifting of some ions of small size to interstitial positions in the crystal lattice after irradiation [16].

XRD patterns of both pristine and irradiated samples are shown in figure 2. The clear inspection of phase identification study of XRD patterned show M-type barium hexagonal ferrite (space group $P6_3/mmc$) with small impurity peaks of $\text{Ba}_2\text{Fe}_6\text{O}_{11}$ for both pristine and irradiated barium hexagonal ferrite samples. It can be seen from figure 2 that the intensity of orthorhombic $\text{Ba}_2\text{Fe}_6\text{O}_{11}$ impurity phase ($a = 23.024 \text{ \AA}$ $b = 5.181 \text{ \AA}$ $c = 8.900$) slightly increases with irradiation compare to main phase. This phenomenon implies that both phases are in equilibrium where irradiation increased the percentage of $\text{Ba}_2\text{Fe}_6\text{O}_{11}$. The lattice parameters $a = 5.892 \text{ \AA}$ and $c = 23.183 \text{ \AA}$ are agreed with JCPDS file—PDF#840757 [17]. It can be said that the basic

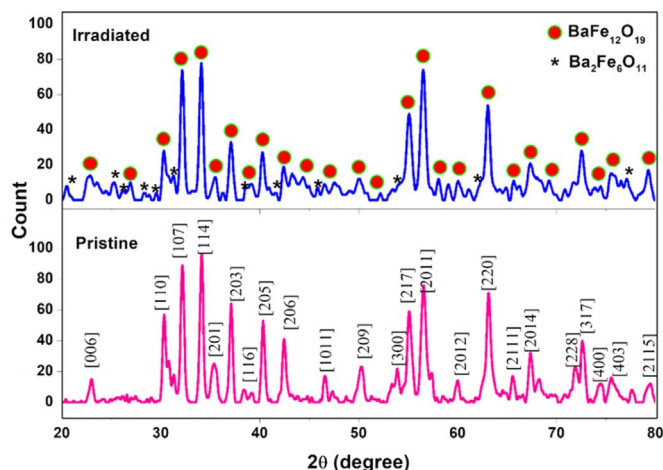


Figure 2. XRD patterns of pristine and irradiated $\text{BaFe}_{12}\text{O}_{19}$ powder along with minor $\text{Ba}_2\text{Fe}_6\text{O}_{11}$ impurity.

Table 1. Lattice constants, unit-cell volume, crystallite size and Magnetic parameters of pristine and irradiated $\text{BaFe}_{12}\text{O}_{19}$ samples.

Parameter	Pristine	Irradiated
Lattice Parameter a (Å)	5.8947	5.8949
Lattice Parameter c (Å)	23.1881	23.1865
c/a ratio	3.9337	3.9333
Unit cell Volume (Å ³)	697.760	697.759
Crystallite size (nm)	41.24	44.58
Saturation Magnetisation M_s (emu g ⁻¹)	55.492	36.789
Remanance Magnetisation M_r (emu g ⁻¹)	30.341	20.317
Coercivity H_c (Oe)	4627	4224

hexagonal crystal structure remains almost the same after irradiation. By the comparison of XRD peaks of the pristine and irradiated barium hexaferrite sample, the widths and peak intensities were altered slightly. The peaks intensity of pristine sample has much higher and sharp with less width than irradiated sample. The irradiation on barium hexaferrite sample origins inelastic collisions of higher energy ions with the molecules and introduces either point defects or partial re-crystallization and track formation in the material, which alter the crystal lattices and the peak intensities [18].

The higher intensity diffraction peaks in XRD pattern of irradiated barium hexaferrite sample clearly indicates that the mean particle size is in the range of nanometers [19, 20]. The crystallite sizes were calculated using the Scherrer's formula using full-width at half maxima (β), wavelength (λ) of x-ray and Bragg angle θ . The lattice constants, unit-cell volume and crystallite size of both pristine and irradiated $\text{BaFe}_{12}\text{O}_{19}$ samples were calculated and the values were given in table 1. There is no much change in lattice constants and unit-cell volume, but crystallite size was found to be increased in the irradiated sample. The c/a ratio is found to be 3.933 in pristine and irradiated barium hexaferrite samples and is in conformity with the reported for M-type hexagonal structure [21, 22]. The increase in crystallite size of barium hexaferrite in present investigation with the irradiation of heavy ions specifies stress-induced defects and distortion in the lattice. However, the nature of substance gets altered for more radiation exposure.

TEM micrographs of pristine and irradiated barium hexaferrite samples is shown in figure 3. The pristine sample shows more uniform grains of cluster with a little agglomeration. However, it is difficult to detect the exact particle size in the irradiated barium hexaferrite samples. TEM images shows that clustering is more in the radiated samples. Swift ion radiation leads to create more cluster in the irradiated $\text{BaFe}_{12}\text{O}_{19}$ sample due the local heat generated during the radiation process. In addition, the particle size of the irradiated barium hexaferrite sample is a higher than that of pristine barium hexaferrite sample. This observation is similar to the observation made for effects of 200 MeV Ag^{15+} ion irradiation on structural properties of nanocrystalline ferrites reported in the literature [20]. The electronic energy loss in nanoparticles was occurred due to inelastic collisions of high energy ions with the host atoms and molecules during the swift heavy ions irradiation. This leads to introduce either point/cluster-like defects/imperfections or partial amorphization depending on the dosage of the radiation and amount of energy lost [21].

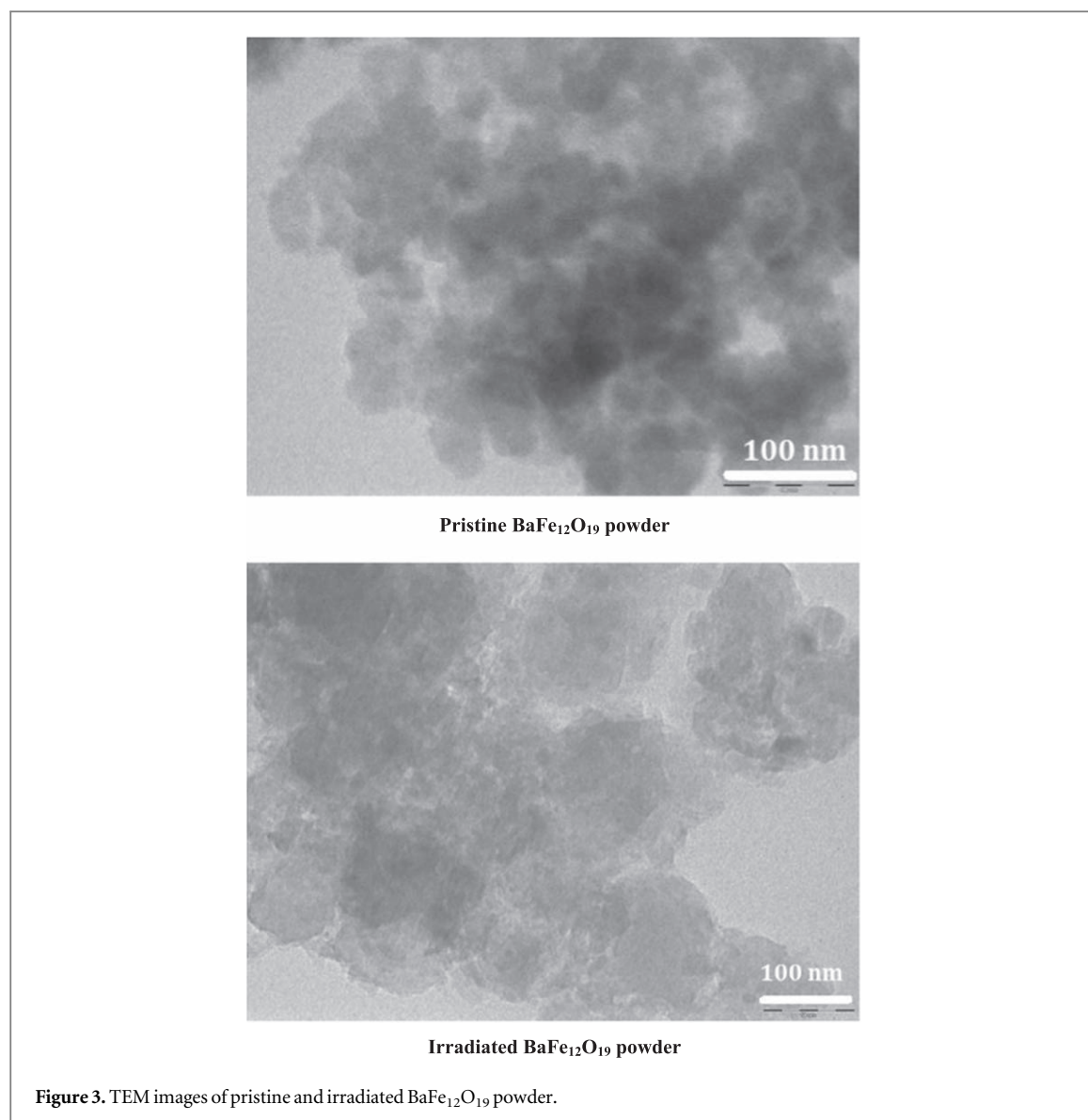


Figure 3. TEM images of pristine and irradiated $\text{BaFe}_{12}\text{O}_{19}$ powder.

Room temperature hysteresis loops of pristine and irradiated barium hexaferrite samples is shown in figure 4. Saturation magnetization (M_s) and coercivity (H_c) of irradiated sample is slightly less than that of pristine sample. From figure 4, the saturation magnetization samples could not be attained for an applied field. Therefore, the values of saturation magnetization were determined by the extrapolation plot of inverse of the applied field and magnetization (M) where H_c is obtained at $1/H = 0$ [23]. As discussed previously, the irradiated hexaferrite samples exhibit cluster and agglomeration of grains (figure 3) easing the flow of applied field through it. Thus coercivity should decrease in the irradiated hexaferrite samples in comparison to the pristine barium hexaferrite and table 1 is in agreement with this variation with H_c of 4227 Oe in irradiated and 4627 Oe in the pristine barium hexaferrite. Similarly, the value of saturation magnetisation decreases from 55.49 to 36.77 emu g^{-1} .

Mosleh *et al* [24] was adopted co-precipitation route to prepare the prepared barium hexa ferrite nano particles. The saturation magnetization varies from 46 to 42.2 emu g^{-1} for the variation of annealing temperature on barium hexaferrites from 900 to 1200 °C. However, the particle size of the particles in the present investigation is very less than earlier reported values. By using the Swift heavy ion irradiation on barium hexaferrites, the magnetization of the pristine samples decreases nearly 33%. The irradiated barium hexaferrite sample shows a smaller magnetization than pristine barium hexaferrite implies, the swift heavy ion-induced disorder. From TEM observation for both pristine and irradiated barium hexaferrite samples, the size of the crystallite/particle is of the order of nanometers and are almost same. Generally, single domain state existed in nanocrystalline sample require higher fields for orientation on applied field direction. These energy-rich Swift heavy ions enter in the sample lead to alteration of atomic ordering by pushing the atoms from their regular position sites. The amorphous tracks were formed during irradiation which was helping to suppress the atomic

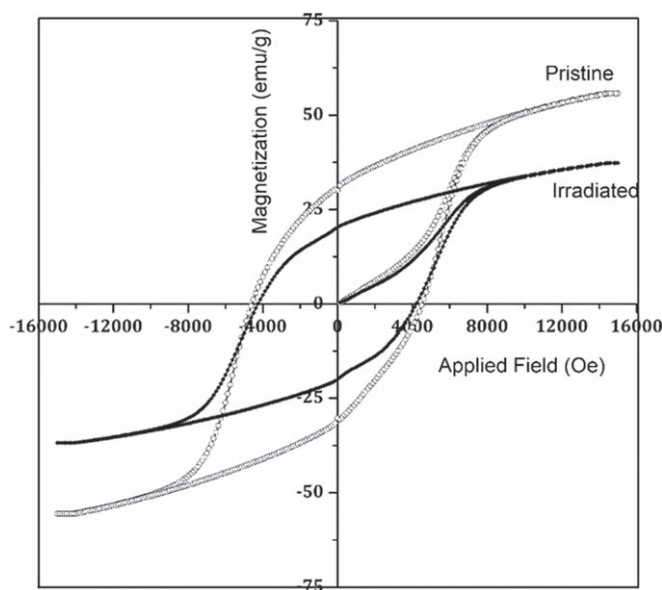


Figure 4. Hysteresis loops of pristine and irradiated BaFe₁₂O₁₉ samples.

and ferrimagnetic long-range ordering [21]. Irradiation disturbs effectively on Fe³⁺ site 4f⁴ (tetrahedral) besides 4f⁴ (octahedral) site than the 12k sites. This phenomenon reduces the superexchange interactions between Fe³⁺–O–Fe³⁺ in the crystallographic site i.e. octahedral as well as tetrahedral site and decreases the magnetization in irradiated sample [8].

The increasing impurity phase of Ba₂Fe₆O₁₁ by irradiation might be one of the reasons of decreasing saturation magnetization. The cause for magnetism in ferrites is indirect exchange interaction between lattice O²⁻ and the magnetic ions [25, 26]. Generally, four building blocks, namely S, S*, R, and R* were used to construct M-type BaFe₁₂O₁₉ [27] hexaferrite. Spinel structure with two oxygen layers with a hexagonal structure with of three oxygen layers were existed in S and S* blocks and R and R* blocks respectively. The BaFe₁₂O₁₉ unit cell contains 38O²⁻, 2Ba²⁺ and 24Fe³⁺ ions [23]. Swift ion irradiation produces more oxygen vacancies through the high density electronic excitation process, and the corresponding density efficiency of Fe³⁺ ions depends on the electronic excitation process [28, 29]. The uniaxial magnetic anisotropy existed in BaFe₁₂O₁₉ hexaferrite was decreased by the oxygen vacancies created by swift ion radiation and hence, the magnetic saturation value was decreased. Due to the similar reason, remenance magnetization also decreases in the sample. Thus, irradiation affects the magnetic character of the sample.

4. Conclusion

M-type barium hexagonal ferrite synthesized via sol-gel auto combustion technique was examined using 200 MeV Ag¹⁶⁺ ion beam on its structural and magnetic nature. Coercivity decreases in the irradiated sample due to the decrease in crystallite and grain size on irradiation. The irradiated sample shows a lower magnetization value than pristine sample due to ion-induced disorder and decreasing of superexchange interactions.

Acknowledgments

We are thankful to Dr. Rajshree B Jotania, Professor, Gujarat University, Ahmedabad 380 009, India, for her guidance and this work is supported by IUAC project (No. IUAC/XIII.3A dated 17-07-2013) and DRS-SAP-I program of UGC (F.530/10/DRS/2010 (SAP-I), 2010), New Delhi, India.

ORCID iDs

K Sakthipandi  <https://orcid.org/0000-0003-3126-0991>

References

- [1] Kaur B, Bhat M, Licci F, Kumar R, Kotru P N and Bamzai K K 2004 *Nucl. Instrum. Methods Phys. Res., Sect. B* **222** 175–86
- [2] Smit J and Wijn H P J 1954 *Advances in Electronics and Electron Physics* vol 6, pp 69–136 (New York: Academic)
- [3] Mane M L, Dhage V N, Shirsath S E, Sundar R, Ranganathan K, Oak S M and Jadhav K M 2013 *J. Mol. Struct.* **1035** 27–30
- [4] Dolia S N, Kumar R, Sharma S K, Sharma M P, Chander S and Singh M 2008 *Curr. Appl Phys.* **8** 620–5
- [5] Singh J P, Dixit G, Srivastava R C, Kumar H, Agrawal H M and Kumar R 2012 *J. Magn. Magn. Mater.* **324** 3306–12
- [6] Ruan S, Xu B, Suo H, Wu F, Xiang S and Zhao M 2000 *J. Magn. Magn. Mater.* **212** 175–7
- [7] Sugimoto S, Kondo S, Okayama K, Nakamura H, Book D, Kagotani T, Homma M, Ota H, Kimura M and Sato R 1999 *IEEE Trans. Magn.* **35** 3154–6
- [8] Kaur B, Bhat M, Kumar R, Kulkarni S D, Joyd P A, Bamzaia K K and Kotru P N 2006 *J. Magn. Magn. Mater.* **305** 392–402
- [9] Shinde S R, Bhagwat A, Patil S I, Ogale S B, Mehta G K, Date S K and Marest G 1998 *J. Magn. Magn. Mater.* **186** 342–8
- [10] Panchal N R and Jotania R B 2013 In *Defect and Diffusion Forum* **341** 155–68 Trans Tech Publications
- [11] Yang N, Yang H, Jia J and Pang X 2007 *J. Alloys Compd.* **438** 263–7
- [12] Tan G and Chen X 2013 *J. Magn. Magn. Mater.* **327** 87–90
- [13] Enidiki A, Juraszek J, Teillet J and Studer F 1999 *Appl. Phys. Lett.* **75** 1296–8
- [14] Li Y, Wang Q and Yang H 2009 *Curr. Appl Phys.* **9** 1375–80
- [15] Ziegler J F and Manoyan J 1988 *Nucl. Instrum. Methods Phys. Res. B* **35** 215–28
- [16] Mane M L, Shirsath S E, Dhage V N and Jadhav K M 2011 *Nucl. Instrum. Methods Phys. Res. B* **269** 2026–31
- [17] Obradors J 1985 *Solid State Chem.* **56** 171
- [18] Khawal H A, Mote V D, Asokan K and Dole B N 2018 *J. Solid State Electr.* **22** 1237–48
- [19] Singh M, Dogra A and Kumar R 2002 *Nucl. Instrum. Methods Phys. Res., Sect. B* **196** 315–23
- [20] Dolia S N et al 2012 *Appl. Surf. Sci.* **258** 4207–11
- [21] Rao B P, Rao K H, Subba Rao P S V, Kumar A M, Murthy Y L N, Asokan K, Siva Kumar V V, Kumar R, Gajbhiye N S and Caltun O F 2006 *Nucl. Instrum. Methods Phys. Res., Sect. B* **244** 27–30
- [22] Wagner T R 1998 *J. Solid State Chem.* **136** 120–4
- [23] Kale A, Gubbala S and Misra R D K 2004 *J. Magn. Magn. Mater.* **277** 350–8
- [24] Mosleh Z, Kameli P, Ranjbar M and Salamati H 2014 *Ceram. Int.* **40** 7279–84
- [25] Singh S and Khare N 2016 *Appl. Surf. Sci.* **364** 783–8
- [26] Lee D, Cho C-W, Kim J W, Bae J-S, Yun H-J, Lee J and Park S 2017 *J. Non-Cryst. Solids* **456** 83–7
- [27] Iqbal M J, Ashiq M N, Hernández-Gómez P, Muñoz J M M and Cabrera C T 2010 *J. Alloys Compd.* **500** 113–6
- [28] d'Orléans C, Stoquert J P, Estournes C, Cerruti C, Grob J J, Guille J L, Haas F, Muller D and Richard-Plouet M 2003 *Phys. Rev. B* **67** 220101
- [29] Shimizu K, Kosugi S, Tahara Y, Yasunaga K, Kaneta Y, Ishikawa N, Hori F, Matsui T and Iwase A 2012 *Nucl. Instrum. Methods Phys. Res., Sect. B* **286** 291–4